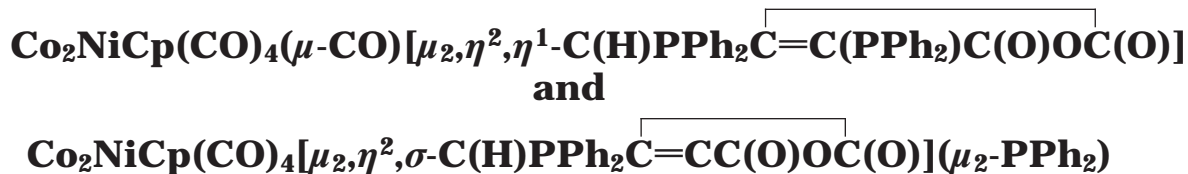


**Phosphine Ligand Attack at Both the Methylidyne Cap
and the CpNi Center in $\text{HCCo}_2\text{NiCp}(\text{CO})_6$ by
2,3-Bis(diphenylphosphino)maleic Anhydride (bma):
P–C Bond Cleavage Reactivity, Kinetics, and X-ray
Structures of the Zwitterionic Clusters**



Simon G. Bott*

Department of Chemistry, University of Houston, Houston, Texas 77204

Kaiyuan Yang, Kathleen A. Talafuse, and Michael G. Richmond*

Department of Chemistry, University of North Texas, Denton, Texas 76203

Received November 7, 2002

Thermolysis of the hydrogen-capped cluster $\text{HCCo}_2\text{NiCp}(\text{CO})_6$ (**1**) with the redox-active diphosphine 2,3-bis(diphenylphosphino)maleic anhydride (bma) in DCE at ca. 80 °C affords the zwitterionic cluster $\text{Co}_2\text{NiCp}(\text{CO})_4(\mu\text{-CO})[\mu_2, \eta^2, \eta^1\text{-C(H)PPh}_2\text{C}=\text{C}(\text{PPh}_2)\text{C(O)OC(O)}]$ (**2**) as the first observable product. Cluster **2** is not stable and transforms into the phosphido-bridged cluster $\text{Co}_2\text{NiCp}(\text{CO})_4[\mu_2, \eta^2, \sigma\text{-C(H)PPh}_2\text{C}=\text{CC(O)OC(O)}](\mu_2\text{-PPh}_2)$ (**3**). Both clusters **2** and **3** have been isolated and characterized in solution by IR and ^{31}P NMR spectroscopies, and the solid-state structures of both **2** and **3** have been determined by X-ray crystallography. Cluster **2** exhibits an open Co_2Ni core having one Co–Co and Co–Ni bond. The bma ligand is attached to the hydrocarbyl and CpNi moieties via the PPh_2 groups, and one of the Co centers is tethered to the π bond of the bma ligand. The opened Co_2Ni core of cluster **3** is structurally similar to **2** and consists of a $\mu_2\text{-PPh}_2$ ligand that spans the Co–Co bond and a Ni–C σ bond resulting from the formal coupling of the maleic anhydride residue with the CpNi moiety. The reaction involving the conversion of **2** to **3** was examined by UV–vis spectroscopy and found to obey first-order kinetics. A rate-limiting step involving dissociative CO loss is supported by the rate retardation in the presence of added CO and the activation parameters ($\Delta H^\ddagger = 31.4 \pm 1.2$ kcal/mol and $\Delta S^\ddagger = 21 \pm 4$ eu). Our studies provide the first structural evidence for the attack of a phosphine ligand on the μ_3 -hydrocarbyl ligand in this genre of tetrahedral cluster and suggest that the nature of the capping CR group and the electrophilicity of the CpNi center play a role in determining the course of ligand substitution. Reactivity comparisons with the related bma-substituted clusters $\text{RCCo}_3(\text{CO})_7(\text{bma})$ are discussed.

Introduction

The ligand substitution chemistry of mononuclear metal compounds with the diphosphine ligands 2,3-bis(diphenylphosphino)maleic anhydride (bma) and 4,5-bis(diphenylphosphino)-4-cyclopenten-1,3-dione (bpcd) has been actively investigated over the past decade. These initial reports have primarily centered on the preparation and characterization of neutral, 18-electron bma- and bpcd-substituted complexes, along with the corresponding 19-electron complexes.^{1–5} Here the added charge density in the 19-electron complex does not populate a metal-based orbital but has been shown by

spectroscopic and MO methods to be localized extensively on the low-lying π^* system belonging to the maleic anhydride and cyclopenten-1,3-dione residues.^{1–3,6} Such

(1) (a) Fenske, D.; Becher, H. *J. Chem. Ber.* **1974**, *107*, 117; **1975**, *108*, 2115. (b) Fenske, D. *Angew. Chem., Int. Ed. Engl.* **1976**, *15*, 381. (c) Fenske, D. *Chem. Ber.* **1979**, *112*, 363. (d) Benschmann, W.; Fenske, D. *Angew. Chem., Int. Ed. Engl.* **1979**, *18*, 677. (e) Fenske, D.; Christidis, A. *Angew. Chem., Int. Ed. Engl.* **1981**, *20*, 129.

(2) (a) Mao, F.; Tyler, D. R.; Keszler, D. *J. Am. Chem. Soc.* **1989**, *111*, 130. (b) Fei, M.; Sur, S. K.; Tyler, D. R. *Organometallics* **1991**, *10*, 419. (c) Mao, F.; Tyler, D. R.; Bruce, M. R. M.; Bruce, A. E.; Rieger, A. L.; Rieger, P. H. *J. Am. Chem. Soc.* **1992**, *114*, 6418. (d) Meyer, R.; Schut, D. M.; Keana, K. J.; Tyler, D. R. *Inorg. Chim. Acta* **1995**, *240*, 405. (e) Schut, D. M.; Keana, K. J.; Tyler, D. R.; Rieger, P. H. *J. Am. Chem. Soc.* **1995**, *117*, 8939.

(3) Yang, K.; Bott, S. G.; Richmond, M. G. *Organometallics* **1995**, *14*, 2387.

* Corresponding authors.

reduced compounds have the ability to function as electron reservoirs and are more accurately referred to as "18 + δ " complexes, where the δ designation serves to indicate the amount of electron density at the metal center in excess of that found for the closed-shell, diamagnetic 18-electron state.⁷

Given the fact that many odd-electron systems show a pronounced reactivity enhancement in terms of ligand substitution and isomerization reactions relative to their 18-electron precursors,^{8,9} the "18 + δ " complexes based on bma and bpcd ligands demonstrated early promise and were attractive models for the quantitative study of the direct effect of δ on the rate of a reaction involving ligand dissociation. Despite the qualitative relationship that exists between the amount of charge density on a metal center and dissociative CO loss in mononuclear bma and bpcd complexes, no linear correlation exists between reaction rates and the surplus electron density at a metal center as measured by the δ parameter. Tyler and Rieger have conclusively proven that the polarity of the reaction solvent and its involvement with the transition state, as manifested by the ΔS^\ddagger contribution of the reaction, negate a simple and direct correlation of δ with the rate for a dissociative ligand loss process.^{2e}

Our interest in the ligands bma and bpcd derives from the coordination chemistry and reactivity of these ligands at di- and polynuclear clusters.^{10–12} Besides the novel coordinative flexibility exhibited by these diphosphines about the cluster polyhedron in terms of ligand isomerism via bridge-to-chelate exchanges, we have also observed the facile activation of the hydrocarbyl capping ligand and the diphosphine ligand.^{11a,12a,13} Oxidative activation of the diphosphine ligand is rapidly followed by a reductive coupling of the hydrocarbyl capping ligand with the transient Co–C σ bond formed from the carbocyclic moiety of the original diphosphine ligand.

(4) Lewis, J. S.; Health, S. L.; Powell, A. K.; Zweit, J.; Blower, P. J. *J. Chem. Soc., Dalton Trans.* **1997**, 855.

(5) Duffy, N. W.; Nelson, R. R.; Richmond, M. G.; Rieger, A. L.; Rieger, P. H.; Robinson, B. H.; Tyler, D. R.; Wang, J. C.; Yang, K. *Inorg. Chem.* **1998**, *37*, 4849.

(6) (a) Tyler, D. R.; Mao, F. *Coord. Chem. Rev.* **1990**, *97*, 119. (b) Tyler, D. R. *Acc. Chem. Res.* **1991**, *24*, 325.

(7) For an early definition of this parameter, see: Brown, T. L. In *Organometallic Radical Processes*; Troglor, W. C., Ed.; Elsevier: New York, 1990; Chapter 3.

(8) (a) Astruc, D. *Electron Transfer and Radical Processes in Transition-Metal Chemistry*; Wiley-VCH: New York, 1995. (b) Kochi, J. K. *J. Organomet. Chem.* **1986**, *300*, 139. (c) Robinson, B. H.; Simpson, J. In *Paramagnetic Organometallic Species in Activation/Selectivity, Catalysis*; Chanon, M.; Julliard, M.; Poite, J. C., Eds.; Kluwer Academic Press: Boston, 1989; p 357.

(9) Klein, A.; Volger, C.; Kaim, W. *Organometallics* **1996**, *15*, 236.

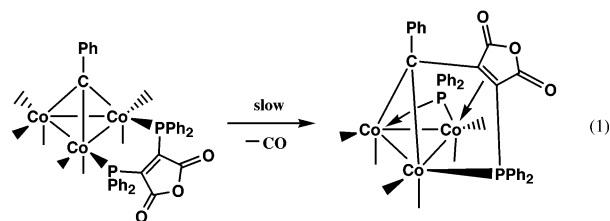
(10) For bma-substituted dinuclear complexes, see: (a) Yang, K.; Bott, S. G.; Richmond, M. G. *Organometallics* **1994**, *13*, 3767; 3788; **1995**, *14*, 4977. (b) Yang, K.; Bott, S. G.; Richmond, M. G. *J. Organomet. Chem.* **1996**, *516*, 65. (c) Bott, S. G.; Yang, K.; Wang, J. C.; Richmond, M. G. *Inorg. Chem.* **2000**, *39*, 6051.

(11) (a) Yang, K.; Smith, J. M.; Bott, S. G.; Richmond, M. G. *Organometallics* **1993**, *12*, 4779. (b) Yang, K.; Bott, S. G.; Richmond, M. G. *Organometallics* **1995**, *14*, 919; 2718. (c) Yang, K.; Martin, J. A.; Bott, S. G.; Richmond, M. G. *Organometallics* **1996**, *15*, 2227. (d) Shen, H.; Bott, S. G.; Richmond, M. G. *Inorg. Chim. Acta* **1996**, *250*, 195. (e) Xia, C.-G.; Yang, K.; Bott, S. G.; Richmond, M. G. *Organometallics* **1996**, *15*, 4480.

(12) (a) Shen, H.; Bott, S. G.; Richmond, M. G. *Organometallics* **1995**, *14*, 4625. (b) Shen, H.; Williams, T. J.; Bott, S. G.; Richmond, M. G. *J. Organomet. Chem.* **1995**, *505*, 1. (c) Bott, S. G.; Wang, J. C.; Shen, H.; Richmond, M. G. *J. Chem. Crystallogr.* **1999**, *29*, 391. (d) Bott, S. G.; Shen, H.; Richmond, M. G. *Struct. Chem.* **2001**, *12*, 225; 237.

(13) For a report involving the P–C bond activation of the bma ligand by a mononuclear complex, see: Bensmann, W.; Fenske, D. *Angew. Chem., Int. Ed. Engl.* **1978**, *17*, 462.

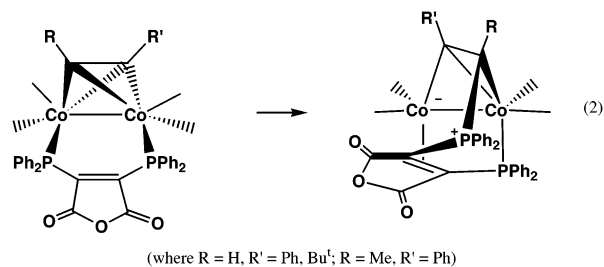
This reaction is illustrated below for $\text{PhCCO}_3(\text{CO})_7(\text{bma})$, which represents our first report on a bma-substituted cluster.



Of interest to us has been the role of the capping carbyne R group and its participation, if any, in the course of the P–C bond/hydrocarbyl ligand activation sequence depicted in eq 1. Whether or not the role played by the R group is entirely steric in helping direct the initial diphosphine ligand activation remains unclear. Thermolysis or photochemical activation of the bma-substituted clusters $\text{PhCCO}_3(\text{CO})_7(\text{bma})$ and $\text{FcCCO}_3(\text{CO})_7(\text{bma})$ has been shown to furnish $\text{Co}_3(\text{CO})_6[\mu_2, \eta^2, \eta^1-$

$\text{C}(\text{R})\text{C}=\text{C}(\text{PPh}_2)\text{C}(\text{O})\text{OC}(\text{O})](\mu\text{-PPh}_2)$.^{11a,d} While the tetrahedrane clusters $\text{RCCO}_3(\text{CO})_7(\text{bma})$ (where R = Me, Cl, CO_2Et) are easily prepared, the thermolysis chemistry of these derivatives does not parallel that of the Ph- and Fc-substituted heptacarbonyl species, which afford relatively high isolated yields of $\text{Co}_3(\text{CO})_6[\mu_2, \eta^2, \eta^1-$

$\text{C}(\text{R})\text{C}=\text{C}(\text{PPh}_2)\text{C}(\text{O})\text{OC}(\text{O})](\mu\text{-PPh}_2)$. Extensive decomposition is observed in $\text{RCCO}_3(\text{CO})_7(\text{bma})$ (where R = H, Me, Cl, CO_2Et) upon thermolysis, unlike the reactions with the Ph- and Fc-capped derivatives.¹⁴ While these data may signal the possible involvement of the capping hydrocarbyl moiety in the decomposition reaction through a phosphine attack path on the carbon center of the μ_3 -CR moiety,¹⁵ we note that more work is required before any gross generalizations regarding the reactivity of this genre of diphosphine at a polynuclear entity can be put forward with certainty. We have previously shown that a phosphine attack on a coordinated alkyne ligand, the isolobal relative of the μ_3 -CR ligand,¹⁶ is a feasible reaction pathway with the alkyne-bridged complexes $\text{Co}_2(\text{CO})_4(\text{bma})(\mu\text{-alkyne})$.^{10a,b} Here thermolysis promotes the attack of one PPh_2 moiety on the least-substituted alkyne carbon atom to furnish the zwitterionic phosphonium complexes shown in eq 2.



Herein we conclusively demonstrate the feasibility of bma ligand attack on the μ_3 -CH moiety through the

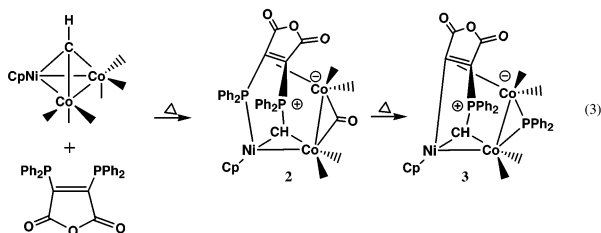
(14) Unpublished results.

(15) For several examples of phosphine ligand attack on μ_3 -ketenylidene and μ_3 -vinylidene ligands in trimetal clusters, see: (a) Ching, S.; Sabat, M.; Shriver, D. F. *Organometallics* **1989**, *8*, 1047. (b) Ching, S.; Jensen, M. P.; Sabat, M.; Shriver, D. F. *Organometallics* **1989**, *8*, 1058. (c) Albiez, T.; Heineke, D.; Vahrenkamp, H. *Chem. Ber.* **1991**, *124*, 1025.

isolation and characterization of $\text{Co}_2\text{NiCp}(\text{CO})_4(\mu\text{-CO})\text{-}[\mu_2, \eta^2, \eta^1\text{-C(H)PPh}_2\text{C}\equiv\text{C(PPh}_2\text{)C(O)OC(O)}]$ (**2**). The thermal instability of **2** and its conversion to the phosphido-bridged cluster $\text{Co}_2\text{NiCp}(\text{CO})_4[\mu_2, \eta^2, \sigma\text{-C(H)PPh}_2\text{C}\equiv\text{CC(O)OC(O)}](\mu_2\text{-PPh}_2)$ (**3**) are verified by kinetic studies and X-ray crystallography. The substitution chemistry and mode of bma ligand reactivity in clusters **1** and **2** are contrasted with the reported chemistry for the homometallic $\text{RCCo}_3(\text{CO})_9$ clusters and bma.

Results and Discussion

I. Thermal Reactivity of $\text{HCCo}_2\text{NiCp}(\text{CO})_6$ with bma and Spectroscopic Data. The mixed-metal cluster $\text{HCCo}_2\text{NiCp}(\text{CO})_6$ (**1**)¹⁷ reacts with added bma in refluxing 1,2-dichloroethane (DCE) to furnish the new blue-green colored cluster $\text{Co}_2\text{NiCp}(\text{CO})_4(\mu\text{-CO})\text{-}[\mu_2, \eta^2, \eta^1\text{-C(H)PPh}_2\text{C}\equiv\text{C(PPh}_2\text{)C(O)OC(O)}]$ (**2**) as the initially observed substitution product. Prolonged heating gradually produces brown-green $\text{Co}_2\text{NiCp}(\text{CO})_4[\mu_2, \eta^2, \sigma\text{-C(H)PPh}_2\text{C}\equiv\text{CC(O)OC(O)}](\mu_2\text{-PPh}_2)$ (**3**) at the expense of the former cluster (vide infra). The best yields of **2** were obtained by following its formation by IR and TLC analyses and terminating the reaction upon ca. 30–45% conversion to **2**. Maximum yields of **3** were realized by heating the reaction overnight. Carrying out the reaction of **1** with bma in refluxing CH_2Cl_2 also afforded **2** and **3** but in rates too slow to be of synthetic importance, and the use of Me_3NO as an oxidative-decarbonylation reagent¹⁸ proved ineffective in promoting the activation of **1** to bma substitution. While we did not explore this latter aspect in detail, we did confirm the decomposition of cluster **1** when treated with Me_3NO . The thermolysis reaction of $\text{HCCo}_2\text{NiCp}(\text{CO})_6$ with bma is shown in eq 3.



Both **2** and **3** were isolated by column chromatography and characterized in solution by spectroscopic methods. Cluster **2** displays terminal $\nu(\text{CO})$ bands 2038 (s), 2003 (s), 1983 (s), and 1962 (w, sh) cm^{-1} , which are of no significant help in determining the mode of bma attachment in **2**. The two carbonyl bands associated with the bma ligand at 1794 (m) and 1728 (m) cm^{-1} are sensitive indicators as to the fate of the bma ligand at a metal cluster. The two bma carbonyl bands are observed at lower energy relative to the free ligand and its simple phosphine-coordinated analogues and suggest

(16) (a) Hoffmann, R. *Angew. Chem., Int. Ed. Engl.* **1982**, *21*, 711. (b) Albright, T. A.; Burdett, J. K.; Whangbo, M. H. *Orbital Interactions in Chemistry*; Wiley: New York, 1985.

(17) Schacht, H. T.; Vahrenkamp, H. *J. Organomet. Chem.* **1990**, *381*, 261.

(18) (a) Koelle, U. *J. Organomet. Chem.* **1977**, *133*, 53. (b) Albers, M. O.; Coville, N. J. *Coord. Chem. Rev.* **1984**, *53*, 227.

that the π bond of the maleic anhydride moiety is coordinated to a cobalt center. The ^{31}P NMR spectrum of $\text{Co}_2\text{NiCp}(\text{CO})_4(\mu\text{-CO})\text{-}[\mu_2, \eta^2, \eta^1\text{-C(H)PPh}_2\text{C}\equiv\text{C(PPh}_2\text{)C(O)OC(O)}]$ exhibits two, relatively sharp ^{31}P doublets at δ 40.71 and 28.91 due to two inequivalent phosphine moieties and immediately rules out the expected cobalt-bridged cluster $\text{HCCo}_2\text{NiCp}(\text{CO})_4(\text{bma})$, the anticipated mode of bma substitution, as depicted in eq 1 for the isolobally related tricobalt clusters $\text{RCCo}_3(\text{CO})_7(\text{bma})$. While the recorded ^{31}P data do not rule out the possibility of cobalt-chelated isomer $\text{HCCo}_2\text{NiCp}(\text{CO})_4(\text{bma})$, the VT ^{31}P NMR behavior of **2** indicates otherwise. The ^{31}P resonances of **2** showed no major line-width variation over the temperature range 176–298 K. These data strongly suggest that the two phosphine groups are not attached to a cobalt center(s) and, therefore, do not experience the commonly observed ^{59}Co quadrupolar broadening of the ^{31}P resonance(s).¹⁹ We tentatively ascribe the lower-field ^{31}P resonance in **2** at δ 40.71 to the phosphonium moiety that is attached to the $\mu_2\text{-CH}$ ligand based on the ^{31}P NMR data reported by us on the zwitterionic hydrocarbyl products shown in eq 2.^{10a,b} There we found that the PPh_2 moiety attached to the alkyne carbon appears ca. 30 ppm downfield relative to the cobalt-substituted phosphine group. Accordingly, the remaining ^{31}P resonance in **2** at δ 28.91 is assigned to the CpNi -bound PPh_2 ligand.

The ^{31}P NMR data for cluster **3** revealed the presence of two ^{31}P singlets at δ 180.27 and 55.34, the former of which is very broad at room temperature and sharpened considerably at 176 K. The full-width at half-height (fwhh) of the latter resonance was insensitive to change as a function of temperature, and this rules out the direct attachment to a cobalt center. These two resonances are readily assigned to a cobalt-bridged μ_2 -phosphido ligand and a phosphonium moiety, the result of PPh_2 attack on the old methylidyne carbon atom, respectively.

II. X-ray Diffraction Data and Molecular Structures for Cluster **2 and **3**.** The molecular structures of **2** and **3** and the disposition of the bma ligand about each cluster polyhedron were determined by X-ray crystallography. Both clusters exist as discrete molecules in the unit cell with no unusually short inter- or intramolecular contacts. The X-ray data and processing parameters are reported in Table 1, with selected bond distances and angles being listed in Table 2.

Figure 1 shows the ORTEP diagram of cluster **2**, and the structural highlights of this 50e cluster rest with the attachment of PPh_2 groups of the bma ligand to the original capping CH group, which furnishes a bridging carbene ligand, and the CpNi center. The electron count at cluster **2** is in excess of that normally found for an electron-precise 48e tetrahedral cluster based on **1**, thus leading to the opening of the Co_2Ni polyhedron. The adopted molecular structure is readily understood within the context of polyhedral skeletal electron pair (PSEP)

(19) For the effects of ^{59}Co broadening on ^{31}P and ^{13}C NMR resonances, see: (a) Yuan, P.; Richmond, M. G.; Schwartz, M. *Inorg. Chem.* **1990**, *30*, 679. (b) Richmond, M. G.; Kochi, J. K. *Organometallics* **1987**, *6*, 254.

Table 1. X-ray Crystallographic Data and Processing Parameters for $\text{Co}_2\text{NiCp}(\text{CO})_4$ -

$(\mu\text{-CO})[\mu_2, \eta^2, \eta^1\text{-C}(\text{H})\text{PPh}_2\text{C}=\text{C}(\text{PPh}_2)\text{C}(\text{O})\text{OC}(\text{O})]$ (**2**)
and $\text{Co}_2\text{NiCp}(\text{CO})_4$ -
 $[\mu_2, \eta^2, \sigma\text{-C}(\text{H})\text{PPh}_2\text{C}=\text{CC}(\text{O})\text{OC}(\text{O})](\mu_2\text{-PPh}_2)$ (**3**)

	2	3
space group	$P2_1/c$, monoclinic	$P2_12_12_1$, orthorhombic
a , Å	9.9456(7)	9.8901(7)
b , Å	18.573(1)	12.228(1)
c , Å	20.753(1)	28.424(4)
β , deg	97.625(6)	
V , Å ³	3799.6(5)	3437.5(6)
mol formula	$\text{C}_{39}\text{H}_{26}\text{Co}_2\text{NiO}_8\text{P}_2$	$\text{C}_{38}\text{H}_{26}\text{Co}_2\text{NiO}_7\text{P}_2$
fw	861.16	833.15
formula units per cell (Z)	4	4
D_{calc} (Mg/m^{-3})	1.504	1.610
λ (Mo $K\alpha$), Å	0.71073	0.71073
abs coeff (mm^{-1})	14.86	16.38
total no. of reflns	5159	1884
no. of ind reflns	1630	965
no. of data/res/params	1630/0/234	965/0/201
R	0.0582	0.0444
R_w	0.0614	0.0500
weights	$[0.04F^2 + (\sigma F)^2]^{-1}$	$[0.04F^2 + (\sigma F)^2]^{-1}$

theory.²⁰ Cluster **1** may be viewed as a four-vertex *nido* cluster with six skeletal electron pairs (SEP), and its reaction with *bma* to give **2** affords a cluster with 8 SEP. The increase in the SEP count on going from **1** to **2** requires an opening of the cluster frame through the formal cleavage of two bonds involved in core bonding (i.e., the Ni–Co and Co– μ_3 -C bonds) and adoption of a *hypho* geometry in **2**. The ancillary $\mu_2, \eta^2, \eta^1\text{-C}(\text{H})\text{PPh}_2\text{C}=\text{C}(\text{PPh}_2)\text{C}(\text{O})\text{OC}(\text{O})$ ligand functions as a 6e donor ligand where the methyldene, maleic anhydride π bond, and the Ni-bound phosphine moieties each act as two-electron-donor groups.

The Ni–Co(1) and Co(1)–Co(2) bond lengths of 2.600(3) and 2.620(3) Å, respectively, are slightly longer than the distances reported for other tetrahedral clusters containing Ni–Co and Co–Co bonds,²¹ but are fully consistent with their single-bond designation. The Ni–Co(1)–Co(2) bond angle of 99.3(1)° agrees well with the value of 97.5(1)° reported by us for the related *hypho*

cluster $\text{Co}_3(\text{CO})_6[\mu_2, \eta^2, \eta^1\text{-C}(\text{Ph})\text{C}=\text{C}(\text{PPh}_2)\text{C}(\text{O})\text{OC}(\text{O})](\mu_2\text{-PPh}_2)$.^{22,23} The formation of the zwitterionic structure in **2** derives from the direct attack of one PPh_2 group on the old μ_3 -CH capping ligand. This gives rise to the phosphonium center P(2) that is charge balanced by a formal negative charge at the Co(2) center through the formal transfer of the bonding electrons from the

(20) (a) Mingos, D. M. P.; Wales, D. J. *Introduction to Cluster Chemistry*; Prentice Hall: Englewoods Cliffs, NJ, 1990. (b) Mingos, D. M. P.; May, A. S. In *The Chemistry of Metal Cluster Complexes*; Shriver, D. F., Kaesz, H. D., Adams, R. D., Eds.; VCH Publishers: New York, 1990; Chapter 2.

(21) (a) Beurich, H.; Blumhofer, R.; Vahrenkamp, H. *Chem. Ber.* **1982**, *115*, 2409. (b) Blumhofer, R.; Fischer, K.; Vahrenkamp, H. *Chem. Ber.* **1986**, *119*, 194. (c) Einstein, F. W. B.; Tyers, K. G.; Tracey, A. S.; Sutton, D. *Inorg. Chem.* **1986**, *25*, 1631.

(22) Yang, K.; Bott, S. G.; Richmond, M. G. *Organometallics* **1995**, *14*, 919.

(23) For related studies that document the reversible polyhedral opening of a tetrahedrane cluster by phosphine addition, see: (a) Planalp, R. P.; Vahrenkamp, H. *Organometallics* **1987**, *6*, 492. (b) Schneider, J.; Minelli, M.; Huttner, G. *J. Organomet. Chem.* **1985**, *294*, 75.

Table 2. Selected Bond Distances (Å) and Angles (deg) in $\text{Co}_2\text{NiCp}(\text{CO})_4(\mu\text{-CO})$ -

$[\mu_2, \eta^2, \eta^1\text{-C}(\text{H})\text{PPh}_2\text{C}=\text{C}(\text{PPh}_2)\text{C}(\text{O})\text{OC}(\text{O})]$ (**2**) and $\text{Co}_2\text{NiCp}(\text{CO})_4[\mu_2, \eta^2, \sigma\text{-C}(\text{H})\text{PPh}_2\text{C}=\text{CC}(\text{O})\text{OC}(\text{O})](\mu_2\text{-PPh}_2)$ (**3**)^a

$\text{Co}_2\text{NiCp}(\text{CO})_4(\mu\text{-CO})[\mu_2, \eta^2, \eta^1\text{-C}(\text{H})\text{-PPh}_2\text{C}=\text{C}(\text{PPh}_2)\text{C}(\text{O})\text{OC}(\text{O})]$ (2)			
Bond Distances			
Ni–Co(1)	2.600(3)	Ni–P(1)	2.154(5)
Co(1)–Co(2)	2.620(3)	Ni–C(1p)	2.16(2)
Ni–C(2p)	2.06(2)	Ni–C(3p)	2.12(2)
Ni–C(4p)	2.10(2)	Ni–C(5p)	2.13(1)
Ni–C(16)	1.96(2)	Co(1)–C(16)	1.99(2)
Co(2)–C(11)	2.00(2)	Co(2)–C(15)	2.00(2)
C(11)–C(15)	1.48(2)	P(2)–C(16)	1.73(2)
Bond Angles			
Co(1)–Ni–P(1)	92.1(1)	P(1)–Ni–C(16)	101.3(5)
Ni–Co(1)–Co(2)	99.3(1)	Ni–Co(1)–C(3)	140.8(6)
Ni–Co(1)–C(16)	48.4(5)	Co(2)–Co(1)–C(3)	46.2(5)
Co(2)–Co(1)–C(16)	93.4(5)	Co(1)–Co(2)–C(3)	46.7(5)
Co(1)–Co(2)–C(11)	97.5(4)	Co(1)–Co(2)–C(15)	93.5(4)
Ni–P(1)–C(11)	115.9(6)	Co(1)–C(3)–Co(2)	87.2(7)
Ni–C(16)–Co(1)	82.4(6)	Ni–C(16)–P(2)	125.1(1)
Co(1)–C(16)–P(2)	113.7(7)		
$\text{Co}_2\text{NiCp}(\text{CO})_4[\mu_2, \eta^2, \sigma\text{-C}(\text{H})\text{PPh}_2\text{C}=\text{CC}(\text{O})\text{OC}(\text{O})](\mu_2\text{-PPh}_2)$ (3)			
Bond Distances			
Ni–Co(1)	2.440(4)	Ni–C(1p)	2.14(2)
Ni–C(2p)	2.12(3)	Ni–C(3p)	2.12(2)
Ni–C(4p)	2.20(2)	Ni–C(5p)	2.11(3)
Ni–C(15)	1.94(2)	Ni–C(16)	1.94(2)
Co(1)–Co(2)	2.585(4)	Co(1)–P(2)	2.189(7)
Co(1)–C(16)	1.94(2)	Co(2)–P(2)	2.173(7)
Co(2)–C(11)	2.01(2)	Co(2)–C(15)	1.98(2)
C(11)–C(15)	1.46(3)		
Bond Angles			
Co(1)–Ni–C(15)	81.5(5)	Co(1)–Ni–C(16)	51.1(6)
Ni–Co(1)–Co(2)	83.4(1)	Ni–Co(1)–P(2)	104.6(2)
Ni–Co(1)–C(16)	50.9(6)	Co(2)–Co(1)–P(2)	53.4(2)
Co(2)–Co(1)–C(16)	96.1(7)	P(2)–Co(1)–C(16)	145.8(7)
Co(1)–Co(2)–P(2)	54.0(2)	Co(1)–Co(2)–C(11)	90.0(5)
Co(1)–Co(2)–C(15)	77.1(5)	P(2)–Co(2)–C(11)	139.1(6)
P(2)–Co(2)–C(15)	103.8(6)	C(11)–P(1)–C(16)	102.0(9)
Co(1)–P(2)–Co(2)	72.7(2)		

^a Numbers in parentheses are estimated standard deviations in the least significant digit.

heterolytically cleaved Co–C bond to the Co(2) center. The *bma* ligand attack on the μ_3 -CH capping ligand is analogous to the process observed by us in a series of $\text{Co}_2(\text{alkyne})(\text{CO})_4(\text{P}-\text{P})$ complexes.^{10a,b} The C(11)–C(15) bond distance of 1.45(2) Å is ca. 0.11 Å longer than the free π bond found in *bma* complexes bound only by the PPh_2 groups. The dihedral angle of ca. 114° formed by the planes defined by the three metal atoms and the maleic anhydride ring shows these groups to be nearly orthogonal, and the near planar arrangement of the P(1)–Ni–Co(1)–Co(2) atoms is evidenced by the a torsion angle of ca. –17°. The remaining bond distances and angles are unexceptional and require no comment.

Figure 2 shows the ORTEP drawing of $\text{Co}_2\text{NiCp}(\text{CO})_4[\mu_2, \eta^2, \sigma\text{-C}(\text{H})\text{PPh}_2\text{C}=\text{CC}(\text{O})\text{OC}(\text{O})](\mu_2\text{-PPh}_2)$. Cluster **3** contains 50e and possesses an open Co_2Ni polyhedral core, and the 8 SEP in **3** lead to the observed *hypho* geometry, as was found in cluster **2**. The ancillary $\mu_2, \eta^2, \sigma\text{-C}(\text{H})\text{PPh}_2\text{C}=\text{CC}(\text{O})\text{OC}(\text{O})](\mu_2\text{-PPh}_2)$ ligand functions collectively as a 5e donor ligand through the

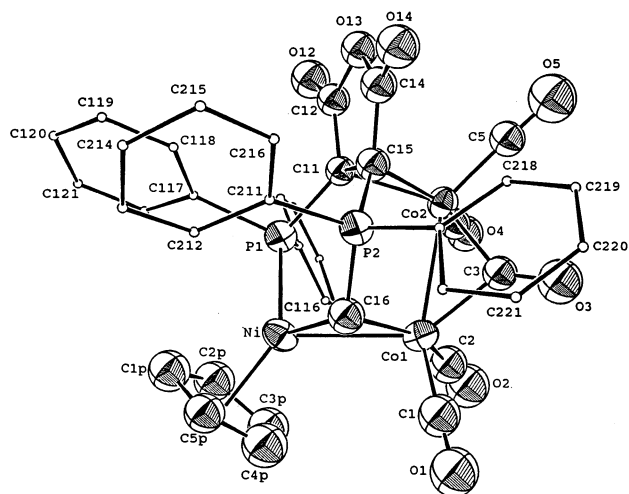


Figure 1. ORTEP drawing of the non-hydrogen atoms of $\text{Co}_2\text{NiCp}(\text{CO})_4(\mu\text{-CO})[\mu_2, \eta^2, \eta^1\text{-C}(\text{H})\text{PPh}_2\text{C}=\text{C}(\text{PPh}_2)\text{C}(\text{O})\text{OC}(\text{O})]$ (**2**) showing the thermal ellipsoids at the 50% probability level.

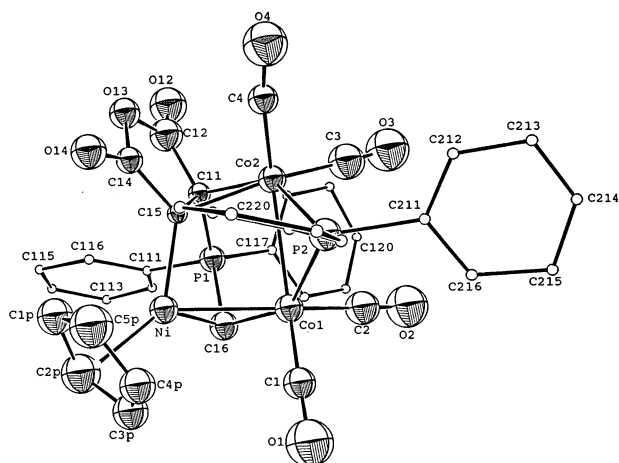


Figure 2. ORTEP drawing of the non-hydrogen atoms of $\text{Co}_2\text{NiCp}(\text{CO})_4[\mu_2, \eta^2, \sigma\text{-C}(\text{H})\text{PPh}_2\text{C}=\text{CC}(\text{O})\text{OC}(\text{O})](\mu_2\text{-PPh}_2)$ (**3**) showing the thermal ellipsoids at the 50% probability level.

bridging of the Ni–Co(1) bond by the methyldene moiety and the maleic anhydride π and σ bonds to the Co and Ni centers, respectively. The phosphido ligand that spans the Co(1)–Co(2) vector in **3** is derived via the P–C cleavage of the P–C(11) bond in **2**. Whether or not this PPh_2 group dissociates from the Ni center in **2** prior to P–C bond activation cannot be assessed at this point.

The Ni–Co(1) [2.440(4) Å] and Co(1)–Co(2) [2.585(4) Å] bond lengths in **3** are in agreement with the single-bond distances found in other mixed-metal NiCo and homometallic Co_3 clusters.^{22,23} The Ni–Co(1)–Co(2) bond angle of 83.43(1)° in **3** is shorter than the corresponding angle found in cluster **2**, and this factor is presumed to be responsible for the shorter metal–metal bond distances in **3** relative to the precursor cluster **2**. The Ni–C(15) σ bond of 1.94(2) Å is consistent with the values recorded for other structurally characterized Ni–C(σ) bonds,²⁴ while the bridging $\mu_2\text{-PPh}_2$ ligand exhibits Co(1)–P(2) and Co(2)–P(2) distances of

Table 3. Experimental Rate Constants for the Reaction of $\text{Co}_2\text{NiCp}(\text{CO})_4(\mu\text{-CO})[\mu_2, \eta^2, \eta^1\text{-C}(\text{H})\text{PPh}_2\text{C}=\text{C}(\text{PPh}_2)\text{C}(\text{O})\text{OC}(\text{O})]$ (**2**) to Give $\text{Co}_2\text{NiCp}(\text{CO})_4[\mu_2, \eta^2, \sigma\text{-C}(\text{H})\text{PPh}_2\text{C}=\text{CC}(\text{O})\text{OC}(\text{O})](\mu_2\text{-PPh}_2)$ (**3**)^a

entry no.	<i>T</i> , °C	$10^4 k_{\text{obsd}}$, s ⁻¹
1	46.6	1.79 ± 0.03
2	52.3	4.14 ± 0.17
3	58.3	7.33 ± 0.19
4	63.3	16.7 ± 0.3
5 ^b	63.3	15.8 ± 0.3
6 ^c	63.3	7.70 ± 0.37
7	69.3	51.4 ± 0.8

^a From 1.74×10^{-4} M $\text{Co}_2\text{NiCp}(\text{CO})_4(\mu\text{-CO})[\mu_2, \eta^2, \eta^1\text{-C}(\text{H})\text{PPh}_2\text{C}=\text{C}(\text{PPh}_2)\text{C}(\text{O})\text{OC}(\text{O})]$ in toluene solvent by following the disappearance of the visible band at 602 nm. All kinetic data reported represent the average of two, independent measurements. ^b From 3.48×10^{-4} M $\text{Co}_2\text{NiCp}(\text{CO})_4(\mu\text{-CO})[\mu_2, \eta^2, \eta^1\text{-C}(\text{H})\text{PPh}_2\text{C}=\text{C}(\text{PPh}_2)\text{C}(\text{O})\text{OC}(\text{O})]$ in toluene. ^c In the presence of 1 atm of CO.

2.189(7) and 2.173(7) Å, respectively, that are normal relative to other $\mu_2\text{-PPh}_2$ -bridged Co–Co bonds.²⁵ The C(11)–C(15) bond distance of 1.46(3) Å is virtually identical to the same linkage found in **2** and confirms the absence of any major destabilizing perturbations for the binding of the maleic ring to the cluster core. The dihedral angle of ca. 63° formed by the planes defined by the three metal atoms and the maleic anhydride ring in cluster **3** reveals that the carbocyclic ring is canted toward the Co(2) center and away from the CpNi and P(1)–Ph groups. The C(15)–Ni–Co(1)–Co(2) atoms display a torsion angle of ca. 5° and are nearly planar. The four ancillary CO groups in cluster **3** are all linear and exhibit bond distances and angles within normally acceptable limits.

III. Kinetic Investigation on the Conversion of **2 to **3**.** Having established the structures of **2** and **3**, we next turned our attention toward examining the relationship between the two clusters. The kinetics for the conversion of **2** to **3** were studied by UV/vis spectroscopy in toluene solution over the temperature range 46.6–69.3 °C by following the change in the absorbance of the 602 nm band of cluster **2**. All reactions exhibited first-order kinetics for at least 4 half-lives, as evidenced by linear plots of $\ln(A_\infty - A_t)$ vs time. The slopes of these plots afforded the first-order rate constants (k_{obsd}) quoted in Table 3. The effect of doubling the initial concentration of **2** and added CO on the reaction is shown by entries 5 and 6, respectively, in Table 3. The reaction of **2** to **3** is retarded by a factor of ca. 2 in the presence of 1 atm of CO. The CO inhibition data along with the observed first-order kinetics and the activation parameters ($\Delta H^\ddagger = 31.4 \pm 1.2$ kcal/mol and $\Delta S^\ddagger = 21 \pm 4$ eu) support a unimolecular process involving dissociative CO as the rate-limiting step that obeys the commonly found rate law:^{26,27}

$$\text{rate} = k_1 k_2 [\text{Co}_2\text{NiCp}(\text{CO})_4(\mu\text{-CO})[\mu_2, \eta^2, \eta^1\text{-C}(\text{H})\text{PPh}_2\text{C}=\text{C}(\text{PPh}_2)\text{C}(\text{O})\text{OC}(\text{O})]] / k_{-1} [\text{CO}] + k_2$$

The observation of CO loss in **2** as a prelude to P–C bond activation and the ultimate formation of **3** has

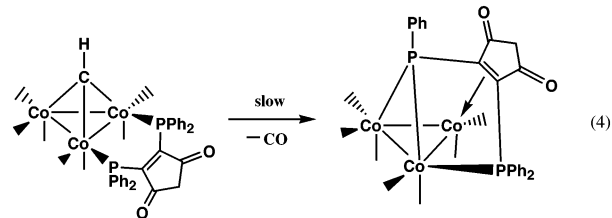
(24) Orpen, A. G.; Brammer, L.; Allen, F. H.; Kennard, O.; Watson, D. G.; Taylor, R. *J. Chem. Soc., Dalton Trans.* **1989**, S1.

been reported by us as a general pathway for diphosphine ligand activation in several bma- and bpcd-substituted systems. The kinetic data indicate that the P–C bond cleavage step must occur at a rate faster than the rates quoted in Table 3.

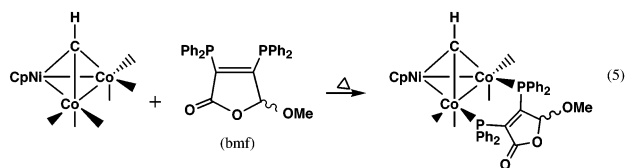
IV. Reactivity Comparison for the Reaction of bma with the Homometallic Clusters $\text{RCCo}_3(\text{CO})_9$ and $\text{HCCo}_2\text{NiCp}(\text{CO})_6$. The normal pattern for CO substitution in $\text{RCCo}_3(\text{CO})_9$ by diphosphine ligands occurs by CO loss and formation of the diphosphine-substituted clusters $\text{RCCo}_3(\text{CO})_7(\text{P}-\text{P})$. Depending upon a variety of factors (bite angle of the P–P ligand, ancillary groups attached to the phosphorus centers, etc.), the typical mode of P–P ligand coordination in $\text{RCCo}_3(\text{CO})_7(\text{P}-\text{P})$ may be either bridging or chelating.²⁸ To our knowledge, no evidence exists for the attack of a P-ligand on the hydrocarbyl capping ligand in this genre of cluster, but this particular course for nucleophilic attack could dominate the reaction if the pathway were governed by a charge-controlled rather than an orbital-controlled manifold.²⁹ The former scenario may be eliminated from consideration based on the MO calculations carried out on $\text{HCCo}_3(\text{CO})_9$ by Fehlner and co-workers,³⁰ where the electronic charge on the $\mu_3\text{-C}$ atom was shown to be substantially negative (ca. -0.40). It is also known that the LUMO in such tetrahedral clusters is essentially an antibonding metal–metal-based orbital of a_2 symmetry containing no hydrocarbyl or capping ligand contribution.³¹

The homometallic clusters $\text{PhCCo}_3(\text{CO})_9$ and $\text{FcCCo}_3(\text{CO})_9$ undergo ligand substitution with bma to produce the expected heptacarbonyl clusters $\text{RCCo}_3(\text{CO})_7(\text{bma})$ (vide supra). We have recently explored the reaction between $\text{HCCo}_3(\text{CO})_9$ and bpcd and find $\text{HCCo}_3(\text{CO})_7(\text{bpcd})$ as the major product from both mild thermolysis and cluster activation by Me_3NO . Thermolysis of this heptacarbonyl cluster gives a low yield of $\text{Co}_3(\text{CO})_7[\mu_2, \eta^2, \eta^1\text{-P}(\text{Ph})\text{C}=\text{C}(\text{PPh}_2)\text{C}(\text{O})\text{CH}_2\text{C}(\text{O})]$,¹⁴ whose structure is shown in eq 4. Despite the fact that the fate of

the methylidyne could not be determined, this reaction has provided us with the first example for the involvement of the methylidyne ligand in the activation of the bpcd ligand.



Our initial assumption concerning the reaction between $\text{HCCo}_2\text{NiCp}(\text{CO})_6$ and bma was that the simple substitution product $\text{HCCo}_2\text{NiCp}(\text{CO})_4(\text{bma})$ would be the major product, in keeping with our data on the homometallic tricobalt clusters and application of the isolobal theory.¹⁶ However, thermolysis reactions of **1** and bma lead only to $\text{Co}_2\text{NiCp}(\text{CO})_4(\mu\text{-CO})[\mu_2, \eta^2, \eta^1\text{-C}(\text{H})\text{PPh}_2\text{C}=\text{C}(\text{PPh}_2)\text{C}(\text{O})\text{OC}(\text{O})]$ (**2**) and $\text{Co}_2\text{NiCp}(\text{CO})_4[\mu_2, \eta^2, \sigma\text{-C}(\text{H})\text{PPh}_2\text{C}=\text{C}(\text{O})\text{OC}(\text{O})](\mu_2\text{-PPh}_2)$ (**3**), without the spectroscopic observation of $\text{HCCo}_2\text{NiCp}(\text{CO})_4(\text{bma})$. The use of Me_3NO failed to produce $\text{HCCo}_2\text{NiCp}(\text{CO})_4(\text{bma})$ under mild conditions, as it has been shown to do in all other tricobalt cluster derivatives examined to date, which would have allowed us to independently explore the follow-up reactions with this suspected intermediate. Unfortunately, the thermolysis conditions required to bring about reaction between $\text{HCCo}_2\text{NiCp}(\text{CO})_6$ and bma to give $\text{HCCo}_2\text{NiCp}(\text{CO})_4(\text{bma})$ are complicated by the subsequent reactions whose rates are faster and produce clusters **2** and **3**. Indirect evidence for the role of $\text{HCCo}_2\text{NiCp}(\text{CO})_4(\text{bma})$ as the initial substitution product comes from the reaction of $\text{HCCo}_2\text{NiCp}(\text{CO})_6$ and the related diphosphine ligand 3,4-bis(diphenylphosphino)-5-methoxy-2(5*H*)-furanone (bmf). Equation 5 illustrates this reaction that gives a diastereomeric mixture of the bmf-bridged isomers.³²



We believe that the thermolysis reaction between $\text{HCCo}_2\text{NiCp}(\text{CO})_6$ and bma initially gives $\text{HCCo}_2\text{NiCp}(\text{CO})_4(\text{bma})$, and the coordinative flexibility of the bma ligand facilitates a series of rearrangements about the cluster polyhedron to ultimately afford cluster **2**.³³ Our extended Hückel MO calculations on $\text{HCCo}_2\text{NiCp}(\text{CO})_6$ reveal interesting data that assist us in our thinking about the course of bma reactivity here. The carbon

(25) (a) Albright, T. A.; Kang, S.-K.; Arif, A. M.; Bard, A. J.; Jones, R. A.; Leland, J. K.; Schwab, S. T. *Inorg. Chem.* **1988**, *27*, 1246. (b) Caffyn, A. J. M.; Mays, M. J.; Solan, G. A.; Conole, G.; Tiripicchio, A. *J. Chem. Soc., Dalton Trans.* **1993**, 2345.

(26) (a) Espenson, J. H. *Chemical Kinetics and Reaction Mechanisms*, 2nd ed.; McGraw-Hill: New York, 1995. (b) Jordan, R. B. *Reaction Mechanisms of Inorganic and Organometallics*; Oxford Press: New York, 1998.

(27) In the absence of added CO ($k_2 > k_{-1}[\text{CO}]$), the rate expression reduces to the simple first-order rate law: rate = $k_1[\text{cluster } 2]$.

(28) (a) Beurich, H.; Vahrenkamp, H. *Chem. Ber.* **1981**, *114*, 2542. (b) Colin, J.; Jossart, C.; Balavoine, G. *Organometallics* **1986**, *5*, 203. (c) Aime, S.; Botta, M.; Gobetto, R.; Osella, D. *J. Organomet. Chem.* **1987**, *320*, 229. (d) Downard, A. J.; Robinson, B. H.; Simpson, J. *Organometallics* **1986**, *5*, 1122, 1132, 1140. (e) Watson, W. H.; Nagl, A.; Hwang, S.; Richmond, M. G. *J. Organomet. Chem.* **1993**, *445*, 163. (f) Yang, K.; Bott, S. G.; Richmond, M. G. *J. Organomet. Chem.* **1993**, *454*, 273. (g) Don, M.-J.; Richmond, M. G.; Watson, W. H.; Krawiec, M.; Kashyap, R. P. *J. Organomet. Chem.* **1991**, *418*, 231.

(29) (a) Klopman, G. *J. Am. Chem. Soc.* **1968**, *90*, 223. (b) Klopman, G. In *Chemical Reactivity and Reaction Paths*; Klopman, G., Ed.; Wiley: New York, 1974; Chapter 4.

(30) DeKock, R. L.; Deshmukh, P.; Dutta, T. K.; Fehlner, T. P.; Housecroft, C. E.; Hwang, J. L.-S. *Organometallics* **1983**, *2*, 1108.

(31) (a) Strouse, C. E.; Dahl, L. F. *J. Am. Chem. Soc.* **1971**, *93*, 6032. (b) Schilling, B. E. R.; Hoffmann, R. *J. Am. Chem. Soc.* **1979**, *101*, 3456. (c) Matheson, T. W.; Peake, B. M.; Robinson, B. H.; Simpson, J.; Watson, D. J. *J. Chem. Soc., Chem. Commun.* **1973**, 894. (d) Peake, B. M.; Robinson, B. H.; Simpson, J.; Watson, D. J. *Inorg. Chem.* **1977**, *16*, 405. (e) Peake, B. M.; Rieger, P. H.; Robinson, B. H.; Simpson, J. *Inorg. Chem.* **1979**, *18*, 1000; **1981**, *20*, 2540. (h) Beurich, H.; Madach, T.; Richter, F.; Vahrenkamp, H. *Angew. Chem., Int. Ed. Engl.* **1979**, *18*, 690.

(32) (a) Unpublished results. (b) The ³¹P NMR spectrum of the diastereomeric mixture of $\text{HCCo}_2\text{NiCp}(\text{CO})_4(\text{bmf})$ reveals the presence of bridging ³¹P chemical shifts at δ 23.5 and 28.4 (73%) and δ 21.8 and 27.2 (27%).

(33) For reports on the ability of cluster-bound phosphines to bridge contiguous metal centers and participate in intramolecular migrations, see: (a) Bradford, A. M.; Douglas, G.; Manojlovic-Muir, L.; Muir, K. W.; Puddephatt, R. J. *Organometallics* **1990**, *9*, 409. (b) Bouherour, S.; Braunstein, P.; R ose, J.; Toupet, L. *Organometallics* **1999**, *18*, 4908. (c) Adams, R. D.; Captain, B.; Fu, W.; Pellechia, P. J. *Chem. Commun.* **2000**, 937. (d) See also refs 10a, b and 11a, d.

atom of the hydrocarbyl capping ligand is negatively charged (−0.24), just as it is in $\text{HCCo}_3(\text{CO})_9$,³⁰ and this should disfavor the direct attack of the phosphine ligand on the hydrocarbyl cap early in the substitution reaction. The MO calculations also revealed that the nickel center has an electronic charge of 0.62, which renders the CpNi moiety electrophilic in nature and susceptible to a charged-controlled attack by the bma ligand at some point in its ambulatory migration about the cluster polyhedron.³⁴ Once the bma ligand has attached itself to the CpNi center, attack at the methylidyne ligand may become feasible. Such ligand direction via a polyhedral metal center merits future research attention.

Conclusions

We have shown that $\text{HCCo}_2\text{NiCp}(\text{CO})_6$ reacts with bma to give $\text{Co}_2\text{NiCp}(\text{CO})_4(\mu\text{-CO})[\mu_2, \eta^2, \eta^1\text{-C}(\text{H})\text{PPh}_2\text{C}=\text{C}(\text{PPh}_2)\text{C}(\text{O})\text{OC}(\text{O})]$ (**2**) as the first observable cluster product, followed by its conversion via a dissociative CO process to furnish $\text{Co}_2\text{NiCp}(\text{CO})_4[\mu_2, \eta^2, \sigma\text{-C}(\text{H})\text{PPh}_2\text{-C}=\text{C}(\text{O})\text{OC}(\text{O})](\mu_2\text{-PPh}_2)$ (**3**). Cluster **2** shows the unusual features of diphosphine ligand attack at the CpNi center and the hydrocarbyl capping ligand that have no parallel in the reaction of $\text{RCCo}_3(\text{CO})_9$ with bma. The precise role played by the capping ligand in the substitution chemistry between the bma ligand and these tetrahedrane clusters is unclear at this time, but our data suggest that the electrophilicity of the CpNi metal center might serve as a site for phosphine attack at some point during phosphine migration about the cluster.

Experimental Section

General Procedures. The $\text{HCCo}_3(\text{CO})_9$ and $\text{BrCCo}_3(\text{CO})_9$ used in the synthesis of $\text{HCCo}_2\text{NiCp}(\text{CO})_6$ were prepared from $\text{Co}_2(\text{CO})_8$ and HCBBr_3 and CBr_4 , respectively.³⁵ The bma ligand was synthesized from 2,3-dichloromaleic anhydride according to the modification described by Tyler,³⁶ and the Cp_2Ni was prepared from anhydrous NiBr_2 , cyclopentadiene, and Et_2NH .³⁷ All reaction and NMR solvents were distilled from an appropriate drying agent under argon and were handled and stored under inert atmosphere using Schlenk techniques.³⁸ The combustion analyses were performed by Atlantic Microlab, Norcross, GA.

Routine infrared spectra were recorded on a Nicolet 20 SXB FT-IR spectrometer in 0.1 mm NaCl cells. The ^{31}P NMR data were recorded on a Varian 300 VXR-300 spectrometer operating at 121 MHz. The reported ^{31}P chemical shifts were referenced to external H_3PO_4 (85%), taken to have $\delta = 0$ and with positive chemical shifts to low field of the external standard.

Synthesis of $\text{HCCo}_2\text{NiCp}(\text{CO})_6$ from $\text{HCCo}_3(\text{CO})_9$. Our procedure followed the general method outlined by Vahren-

(34) Such bma ligand fluxionality is suggested by the facile bridge-to-chelate ligand exchange observed in several bma-substituted dinuclear and polynuclear complexes by VT FT-IR (unpublished data) and ^{31}P NMR measurements (1D and 2D techniques).

(35) (a) Seyferth, D.; Nestle, M. O.; Hallgren, J. S. *Inorg. Synth.* **1980**, *20*, 224. (b) Seyferth, D.; Hallgren, J. S.; Hung, P. L. K. *J. Organomet. Chem.* **1973**, *50*, 265.

(36) Mao, F.; Philbin, C. E.; Weakley, T. J. R.; Tyler, D. R. *Organometallics* **1990**, *9*, 1510.

(37) King, R. B. *Organometallic Syntheses*; Academic Press: New York, 1965; Vol. 1.

(38) Shriver, D. F. *The Manipulation of Air-Sensitive Compounds*; McGraw-Hill: New York, 1969.

kamp, with minor modification as described. To a Schlenk flask under CO was added 2.00 g (4.53 mmol) of $\text{HCCo}_3(\text{CO})_9$ and 50 mL of THF, after which the vessel was charged with 1.50 g (7.95 mmol) of nickelocene. The reaction solution was heated at 65–70 °C for 3 days, with monitoring by TLC analysis. After 3 days, a 1:1 mixture of $\text{HCCo}_3(\text{CO})_9$ and $\text{HCCo}_2\text{NiCp}(\text{CO})_6$ was observed, in addition to a large amount of decomposition, as evidenced by the material that remained at the origin of the TLC plate. The solvent was removed under vacuum, and the desired Co_2Ni cluster was isolated by column chromatography over silica gel using petroleum ether as the eluent. $\text{HCCo}_2\text{NiCp}(\text{CO})_6$ was obtained as a black oily solid. Yield: 18.3% (0.35 g). IR (hexane): $\nu(\text{CO})$ 2077 (s), 2040 (vs), 2024 (vs), 2013 (s) cm^{-1} . The product cluster appears to be temperature sensitive, decomposing over the course of a few days when kept at room temperature under argon. Therefore, we routinely prepared this cluster and employed it immediately in syntheses of clusters **2** and **3**. $\text{HCCo}_2\text{NiCp}(\text{CO})_6$ may, however, be stored under CO in the freezer without significant decomposition for a period of weeks.

Synthesis of $\text{HCCo}_2\text{NiCp}(\text{CO})_6$ from $\text{BrCCo}_3(\text{CO})_9$. The reaction conditions employing $\text{BrCCo}_3(\text{CO})_9$ are identical to those described for the hydrogen-capped cluster above except that the reaction was run under an argon atmosphere. Stirring the reaction solution overnight at 65–70 °C afforded a 3:7 mixture of $\text{HCCo}_3(\text{CO})_9$ and $\text{HCCo}_2\text{NiCp}(\text{CO})_6$. The reaction was terminated and purified by column chromatography. Yield of **1**: 44.5% (0.85 g).

Synthesis of $\text{Co}_2\text{NiCp}(\text{CO})_4(\mu\text{-CO})[\mu_2, \eta^2, \eta^1\text{-C}(\text{H})\text{PPh}_2\text{-C}=\text{C}(\text{PPh}_2)\text{C}(\text{O})\text{OC}(\text{O})]$ and $\text{Co}_2\text{NiCp}(\text{CO})_4[\mu_2, \eta^2, \sigma\text{-C}(\text{H})\text{-PPh}_2\text{C}=\text{C}(\text{O})\text{OC}(\text{O})](\mu_2\text{-PPh}_2)$. To a Schlenk tube containing 0.20 g (0.47 mmol) of $\text{HCCo}_2\text{NiCp}(\text{CO})_6$ in 30 mL of DCE was added 0.27 g (0.56 mmol) of bma, after which the solution was heated at 83 °C for 1 h. TLC examination (7:3 mixture of CH_2Cl_2 /petroleum ether) of the reaction solution at this time revealed a trace of $\text{HCCo}_2\text{NiCp}(\text{CO})_6$ ($R_f = 0.75$), a blue spot corresponding to cluster **2** ($R_f = 0.30$), and a brown spot belonging to cluster **3** ($R_f = 0.20$). The DCE was removed under vacuum, and the products were isolated by column chromatography over silica gel. Use of petroleum ether as the eluent afforded unreacted **1**, after which a 3:1 mixture of CH_2Cl_2 /petroleum was employed as the eluting solvent to give cluster **2**. Cluster **3** was finally isolated when pure CH_2Cl_2 was used as the eluent. Single crystals of **2** and **3** suitable for X-ray diffraction analysis and samples suitable for combustion analysis were grown as CH_2Cl_2 solutions of each cluster that had been layered with hexane. Yield of **2**: 0.11 g (26.8%). IR (CH_2Cl_2): $\nu(\text{CO})$ 2038 (s), 2003 (s), 1983 (s), 1962 (w, sh), 1794 (m, asym bma C=O), 1728 (m, sym bma C=O) cm^{-1} . $^{31}\text{P}\{^1\text{H}\}$ NMR (THF, 178 K): δ 40.71 (1P, $J_{\text{P-P}} = 14.5$ Hz), 28.91 (1P, $J_{\text{P-P}} = 14.5$ Hz). Anal. Calcd (found) for $\text{C}_{39}\text{H}_{26}\text{Co}_2\text{NiO}_8\text{P}_2$: C, 54.39 (54.13); H, 3.04 (3.15). Yield of **3**: 0.13 g (33.0%). IR (CH_2Cl_2): $\nu(\text{CO})$ 2034 (s), 2005 (vs), 1985 (s), 1967 (sh), 1781 (m, asym bma C=O), 1728 (m, sym bma C=O) cm^{-1} . $^{31}\text{P}\{^1\text{H}\}$ NMR (THF, 178 K): δ 180.27 (1P, phosphido), 55.34 (1P, CpNiP). Anal. Calcd (found) for $\text{C}_{38}\text{H}_{26}\text{Co}_2\text{NiO}_7\text{P}_2$: C, 54.78 (54.74); H, 3.15 (3.22).

X-ray Diffraction Structures of $\text{Co}_2\text{NiCp}(\text{CO})_4(\mu\text{-CO})[\mu_2, \eta^2, \eta^1\text{-C}(\text{H})\text{PPh}_2\text{C}=\text{C}(\text{PPh}_2)\text{C}(\text{O})\text{OC}(\text{O})]$ and $\text{Co}_2\text{NiCp}(\text{CO})_4[\mu_2, \eta^2, \sigma\text{-C}(\text{H})\text{PPh}_2\text{C}=\text{C}(\text{O})\text{OC}(\text{O})](\mu_2\text{-PPh}_2)$. X-ray crystals of **2** and **3** suitable for diffraction analysis were selected and sealed inside a Lindemann capillary, followed by mounting on the goniometer of an Enraf-Nonius CAD-4 diffractometer that employed Mo $K\alpha$ radiation. Intensity data in the range $2.0^\circ \leq 2\theta \leq 44^\circ$ (cluster **2**) and $2.0^\circ \leq 2\theta \leq 40^\circ$ (cluster **3**) were collected at room temperature using the ω -scan technique in the variable-scan speed mode and were corrected for Lorentz, polarization, and absorption. The structure of **2** was solved by using SHELX-86, while the structure of **3** was solved

by using SIR. In the case of cluster **2**, the Ni, Co, and P atoms were refined anisotropically. All other non-hydrogen atoms were refined isotropically. Refinement for **2** on F converged at $R = 0.0582$ and $R_w = 0.0614$ for 1630 unique reflections with $I > 3\sigma(I)$. All non-hydrogen atoms in cluster **3** were refined isotropically. The refinement for **3** converged at $R = 0.0444$ and $R_w = 0.0500$ for 965 unique reflections with $I > 3\sigma(I)$ due to the paucity of data.

Kinetic Studies. All kinetic studies involving the conversion of **2** to **3** were monitored spectrophotometrically by using a Hewlett-Packard 8452A UV-vis spectrometer equipped with a variable-temperature cell. The extent of the reaction was determined by following the UV-vis changes in the 602 nm band of **2** for at least 4 half-lives. A VWR refrigerated constant temperature circulator was used to maintain a constant temperature, to within ± 0.2 °C. Plots of $\ln(A_\infty - A_t)$ vs time were linear and gave the first-order rate constants (k_{obsd}) shown in Table 3. The quoted activation parameters were calculated via the Eyring equation.³⁹

Extended Hückel MO Calculations. The calculations on cluster **1** were carried out with the program originally devel-

oped by Hoffmann⁴⁰ and modified by Mealli and Proserpio.⁴¹ The input Z-matrix for $\text{HCCo}_2\text{NiCp}(\text{CO})_6$ was confined to C_s symmetry and utilized bond distances and angles from the X-ray structures of the related clusters $\text{RCCo}_2\text{NiCp}(\text{CO})_6$. The C-H bond distance for the methyldyne ligand was set at 1.05 Å.

Acknowledgment. Financial support from The Robert A. Welch Foundation (B-1093-MGR) is gratefully acknowledged.

Supporting Information Available: Textual presentations of the crystallographic and experimental details, listings of crystallographic data, bond distances, bond angles, and atomic and thermal parameters of $\text{Co}_2\text{NiCp}(\text{CO})_4(\mu\text{-CO})[\mu_2, \eta^2, \eta^1\text{-C(H)PPh}_2\text{C}=\text{C}(\text{PPh}_2)\text{C}(\text{O})\text{OC}(\text{O})]$ (**2**) and $\text{Co}_2\text{NiCp}(\text{CO})_4[\mu_2, \eta^2, \sigma\text{-C(H)PPh}_2\text{C}=\text{CC}(\text{O})\text{OC}(\text{O})](\mu_2\text{-PPh}_2)$ (**3**). This material is available free of charge via the Internet at <http://pubs.acs.org>.

OM0209273

(39) Carpenter, B. K. *Determination of Organic Reaction Mechanisms*; Wiley-Interscience: New York, 1984.

(40) (a) Hoffmann, R.; Lipscomb, W. N. *J. Chem. Phys.* **1962**, *36*, 2179, 3489. (b) Hoffmann, R. *J. Chem. Phys.* **1963**, *39*, 1397.

(41) Mealli, C.; Proserpio, D. M. *J. Chem. Educ.* **1990**, *67*, 399.